Alexander-disease mutation of *GFAP* causes filament disorganization and decreased solubility of GFAP

Victoria C. Hsiao[1], Rujin Tian[1], Heather Long[2], Ming Der Perng[2], Michael Brenner[3], Roy A. Quinlan[2] and James E. Goldman[1,*]

[1]Department of Pathology and the Center for Neurobiology and Behavior, Columbia University, New York, NY 10032, USA
[2]School of Biological and Medical Sciences, University of Durham, Durham, DH1 3LE, UK
[3]Department of Neurobiology, and The Civitan International Research Center, University of Alabama at Birmingham, Birmingham, AL 35294, USA
*Author for correspondence (e-mail: jeg5@columbia.edu)

Accepted 31 January 2005
Journal of Cell Science 118, 2057-2065 Published by The Company of Biologists 2005
doi:10.1242/jcs.02339

Summary

Alexander disease is a fatal neurological illness characterized by white-matter degeneration and the formation of astrocytic cytoplasmic inclusions called Rosenthal fibers, which contain the intermediate filament glial fibrillary acidic protein (GFAP), the small heat-shock proteins HSP27 and αB-crystallin, and ubiquitin. Many Alexander-disease patients are heterozygous for one of a set of point mutations in the *GFAP* gene, all of which result in amino acid substitutions. The biological effects of the most common alteration, R239C, were tested by expressing the mutated protein in cultured cells by transient transfection. In primary rat astrocytes and Cos-7 cells, the mutant GFAP was incorporated into filament networks along with the endogenous GFAP and vimentin, respectively. In SW13Vim$^-$ cells, which have no endogenous cytoplasmic intermediate filaments, wild-type human GFAP frequently formed filamentous bundles, whereas the R239C GFAP formed 'diffuse' and irregular patterns. Filamentous bundles of R239C GFAP were sometimes formed in SW13Vim$^-$ cells when wild-type GFAP was co-transfected. Although the presence of a suitable coassembly partner (vimentin or GFAP) reduced the potential negative effects of the R239C mutation on GFAP network formation, the mutation affected the stability of GFAP in cells in a dominant fashion. Extraction of transfected SW13Vim$^-$ cells with Triton-X-100-containing buffers showed that the mutant GFAP was more resistant to solubilization at elevated KCl concentrations. Both wild-type and R239C GFAP assembled into 10 nm filaments with similar morphology in vitro. Thus, although the R239C mutation does not appear to affect filament formation per se, the mutation alters the normal solubility and organization of GFAP networks.

Key words: Intermediate filaments, Alexander disease, GFAP, Cytoskeleton

Introduction

Alexander disease was first reported in 1949 in a 15-month-old patient with megalencephaly, hydrocephaly and psychomotor retardation (Alexander, 1949). Since then, many more cases have been described in patients of various ages (Borrett and Becker, 1985; Duckett et al., 1992; French et al., 1976; Reichard et al., 1996; Sawaishi et al., 1999) (see http://www.waisman.wisc.edu/alexander/index.html for a literature summary). Clinically, Alexander disease is a fatal leukoencephalopathy that leads to the dysmyelination or demyelination of the central nervous system. At a microscopic level, Alexander disease is characterized by a failure of myelination in infantile cases and a loss of myelin in older patients. A major pathological hallmark is the formation of Rosenthal fibers in astrocytes (Borrett and Becker, 1985; Henin et al., 1986). In Alexander disease, Rosenthal fibers are found throughout the brain and spinal cord, accumulating particularly in astrocyte end-feet in the subpial and perivascular zones (Friede, 1989). They are composed of glial fibrillary acidic protein (GFAP), the major intermediate filament of astrocytes, as well as ubiquitin and the small heat-shock proteins HSP27 and αB-crystallin (Bettica and Johnson, 1990; Goldman and Corbin, 1988; Iwaki et al., 1989; Johnson and Bettica, 1989; Lowe et al., 1989; Tomokane et al., 1991). At the electron-microscopic level, Rosenthal fibers are dense, osmiophilic structures that are closely associated with intermediate filaments (Herndon et al., 1970; Lach et al., 1991).

Many patients with Alexander disease have been found to have one of a series of mutations in the *GFAP* gene (Aoki et al., 2001; Brenner et al., 2001; Gorospe et al., 2002; Okamoto et al., 2002; Rodriguez et al., 2001; Sawaishi et al., 2002; Shiihara et al., 2002; Shiroma et al., 2001) (for a review, see Li et al., 2002). The predicted amino acid changes are scattered throughout the protein, but occur principally in the rod domains, which are crucial for polymerization of GFAP into filaments. Because all of the patients are heterozygous for the mutations, the effects of the mutations appear to be dominant over the wild type. An understanding of the effects of these mutations on GFAP polymerization and organization might elucidate the cellular basis for Rosenthal-fiber formation and the pathophysiology of Alexander disease.

We present a study of the most common mutation, R239C (nucleotide mutation C715T), which produces a severe form of Alexander disease (for a review, see Li et al., 2002). Of the 57

Alexander-disease patients published to date, 18 (32%) have the mutation at R239: 13 have the R239C mutation, four have an R239H mutation and one has an R239P mutation. Patients with an R239 mutation are among the more severely affected, having both an early age of symptom onset (about 10.4 months) and a rapidly progressive disease (Rodriguez et al., 2001; Li et al., 2002). R239 is in the 2a α-helical subdomain of the rod domain, which is highly conserved among species (Brenner et al., 1990; Li et al., 2002).

We have tested the properties of the R239C mutation both by in vitro assembly and by transient transfection into three kinds of cultured cells: primary rat astrocytes, which contain endogenous GFAP and vimentin; Cos-7 cells, which contain endogenous vimentin; and SW13Vim$^-$ cells, which do not contain any cytoplasmic intermediate filaments (Hedberg and Chen, 1986). The mutant GFAP forms 10 nm filaments during in vitro assembly and is incorporated into the existing intermediate filament networks in the primary astrocytes and Cos-7 cells. However, the mutant is unable to form a normal filamentous network by itself in the SW13Vim$^-$ line. Furthermore, mutant GFAP is more resistant to salt extraction than the wild type.

Materials and Methods

Plasmids

The C715T mutation was introduced into a pRSVi plasmid (Chin and Liem, 1989) encoding human full-length GFAP using PCR site-directed mutagenesis. Briefly, sense and antisense PCR oligonucleotides containing the mutation were used with flanking primers to generate a mutated DNA fragment with unique restriction sites. Following digestion, this fragment was then ligated back into the original plasmid, which had been digested with the same enzymes. The entire sequence of the substituted fragment, including the presence of the mutation, was confirmed by sequencing.

Cell culture

Primary astrocytes were cultured from neonatal Sprague-Dawley rat forebrain using a method described previously (Head et al., 1994). 7-10 days after establishing cultures, microglia and progenitors were removed by shaking at 250 rpm, 37°C, for 14-18 hours. Primary astrocytes were grown in Minimal Essential Medium (Gibco BRL, Grand Island, NY) supplemented with 10% fetal bovine serum (FBS; Gibco BRL), 0.5% glucose, MEM Vitamin Solution (Gibco BRL), 200 μM L-glutamine, 100 units ml^{-1} penicillin, 100 μg ml^{-1} streptomycin, 250 ng ml^{-1} amphotericin, pH 7.2-7.3.

Cos-7 and SW13Vim$^-$ cells were a generous gift from R. Liem (Columbia University). They were grown in Dulbecco's modified Eagle's medium (Gibco BRL) supplemented with 1 mM sodium pyruvate and either 10% FBS (Cos-7) or 5% FBS (SW13Vim$^-$), and antibiotics as above. To avoid Vim$^+$ revertants, SW13Vim$^-$ cells were used only at passage numbers less than 12 following an initial selection process and were periodically tested for the presence of vimentin. All cells were kept at 37°C in 5% CO_2.

Transfection

For immunofluorescence, primary cells were plated at 5×10^4 cells per well on poly-L-lysine-coated glass coverslips in 24-well plates. Cos-7 and SW13Vim$^-$ cells were plated at 2×10^4 cells per well or 1×10^4 cells per well for staining 1 day or 3 days after transfection, respectively. The day after plating, cells were transfected with 0.4 μg plasmid using Lipofectamine Plus (Gibco BRL) for 6 hours, after which 1 ml of growth medium was added to each well.

For western blotting, SW13Vim$^-$ cells were plated on tissue-culture dishes at 6.4×10^5 cells per 60 mm dish for extraction 1 day after transfection. Cells were transfected with 2 μg plasmid using Lipofectamine Plus for 6 hours, after which 1.5 ml of growth medium was added.

Indirect immunofluorescence

1 day or 3 days after transfection, cells on coverslips were washed twice with PBS, fixed with 4% w/v paraformaldehyde in PBS for 30 minutes and permeabilized with 0.2% Triton X-100 for 3 minutes at room temperature. Primary antibodies were diluted in 5% normal goat serum in PBS. Primary antibodies used were anti-panGFAP (ALD10, 1:500, rabbit polyclonal) (Goldman and Chiu, 1984) and anti-human-GFAP (SMI21, 1:5000, mouse IgG1; Sternberger Monoclonals, Baltimore, MD). Secondary antibodies used were FITC-conjugated goat anti-mouse-IgG1 (1:50; Southern Biotechnology Associates, Birmingham, AL) and FITC-conjugated goat anti-rabbit (1:200; Chemicon). Primary and secondary antibody incubations were for 1 hour each at room temperature. Coverslips were then mounted onto slides with Gel/Mount (Biomeda, Foster City, CA) supplemented with 0.2% DABCO (Sigma, St Louis, MO). Cells were visualized using an Olympus BX60 microscope or Zeiss LSM 410 confocal microscope.

For statistical analysis, up to four coverslips from two independent experiments were counted for each condition using the Olympus BX60 microscope at a magnification of 100×. Between 102 and 272 transfected cells were counted per coverslip. The cells were distributed into five possible phenotypes: filamentous network alone; filamentous network superimposed on a 'diffuse' background; 'diffuse' pattern alone; irregular pattern superimposed on a 'diffuse' background; and irregular pattern with a filamentous network. We performed a statistical analysis on the proportion of each phenotype found in each plasmid's transfections. Student's *t* test was applied to the difference between two means to compare the results between a pair of different plasmids (Rosner, 1990).

Gel electrophoresis and western blotting

Cells were washed twice with PBS and then extracted with 0.5% v/v Triton X-100, 2 mM Tris-HCl, 2 mM EDTA, 2 mM phenylmethylsulfonyl fluoride, pH 7.0, on ice for 15 minutes (Goldman and Abramson, 1990). For high-salt extractions, KCl was added to the extraction buffer to a final concentration of 0.5 M or 1.0 M. The extracts were spun in a microfuge at 4°C for 10 minutes at 16,000 ***g***. The supernatants ('soluble fraction') were removed and the pellets ('insoluble fraction') were resuspended in 2% w/v SDS, 2 mM Tris-HCl, 2 mM EDTA, pH 6.8, and then boiled for 30 minutes (Goldman and Abramson, 1990). Protein concentrations were determined using the BCA Protein Assay kit (Pierce, Rockford, IL). For the 0.5% v/v Triton X-100, 0 M KCl gel, 20 μg protein each from the soluble and insoluble fractions were diluted in sample buffer (1% SDS, 50 mM Tris-HCl, pH 6.8, 5% glycerol, 0.05% w/v bromophenol blue, 0.25% v/v β-mercaptoethanol), boiled and separated by SDS-PAGE using 11% w/v polyacrylamide gels. For the 0.5 M KCl samples, 15 μg of each fraction were loaded; for the 1.0 M KCl gel, 11 μg of each fraction were used. Electrophoresis was followed by western blotting using wet transfer onto nitrocellulose. The blots were blocked in 5% w/v non-fat milk, 0.1% v/v Tween-20 in PBS (PBS-BT). Blots were stripped by three 10-minute washes of 0.2 M glycine, 1 mM EGTA, pH 2.8, at 37°C, followed by three 10-minute washes with PBS-Tween (PBS-T) at room temperature and reblocking with PBS-BT. A monoclonal anti-panGFAP primary antibody (Chemicon) was used at a 1:10,000 dilution in Blotto [5% (w/v) nonfat dry milk] overnight at 4°C or at a 1:5000 dilution in Blotto for 4 hours at room temperature. Monoclonal AC-40 anti-actin antibody (Sigma) was used at 1:1000 in Blotto overnight at 4°C.

Horseradish-peroxidase-conjugated anti-mouse secondary antibody was used at 1:1000 in PBS-T for 1 hour at room temperature. Bands were visualized with Enhanced Chemiluminescence (ECL) (Amersham, Arlington Heights, IL) on blue X-ray film (Lab Scientific, Livingston, NJ).

Bacterial expression of GFAP

The expression constructs of both wild-type and mutant GFAP were transformed into *Escherichia coli* BL21 (DE3) pLysS strain. Recombinant protein expression was induced using 0.5 mM isopropyl-1-thio-β-D-galactopyranoside for 4 hours once the bacterial culture had reached an optical density at 600 nm of 0.6. GFAP localized to the inclusion body fraction and was purified as described by DEAE ion-exchange chromatography on Fractogel medium (Ralton et al., 1994).

Intermediate-filament assembly and sedimentation assay

In vitro co-sedimentation assays were carried out as previously described (Perng et al., 1999). Briefly, purified GFAP in urea buffer (8 M urea, 20 mM Tris-HCl, pH 8.0, 5 mM EDTA, 2 mM EGTA, 1 mM dithiothreitol) was dialysed by stepwise lowering of the urea concentration into low ionic strength buffer (10 mM Tris-HCl, pH 7.0, 1 mM dithiothreitol) at 4°C. Wild-type or mutant GFAP was assembled by the dialysis method (Perng et al., 1999). Protein samples were then layered onto a 0.85 M sucrose cushion in the assembly buffer and centrifuged at 80,000 ***g*** for 30 minutes at 20°C to pellet GFAP filaments. Fractions were separated by SDS-PAGE on 12% w/v polyacrylamide gels and the proteins in both the supernatant and pellet fractions visualized by Coomassie Blue staining.

Electron microscopy

Protein samples were diluted to 1 mg ml^{-1} and negatively stained with 1% (w/v) uranyl acetate. Samples on carbon-coated copper grids were examined in a Phillips 400T transmission electron microscope, using an accelerating voltage of 80 kV. Images were captured at a magnification of 17,000× on Kodak 4489 film, which were digitized at 1200×1200 pixel resolution and then processed further in Adobe® Photoshop 6 (Adobe Systems, San Jose, CA).

Results

Intermediate-filament organization in primary astrocytes, Cos-7 cells and SW13Vim⁻ cells

We first examined the effect of expressing the wild-type and the mutant human GFAP in primary rat astrocytes by transient transfections. Transfected cells were distinguished from untransfected cells by staining with a human-specific anti-GFAP antibody. Most cells transfected with either construct contained a filamentous GFAP network (Fig. 1A), whereas a minority had large cytoplasmic aggregates (Fig. 1B,C). Both filamentous and aggregate GFAP distributions, the latter consisting of swirls of 10 nm filaments, were previously seen after transfection of wild-type GFAP into astrocytes (Koyama and Goldman, 1999), suggesting that formation of GFAP aggregates is probably due to elevated expression rather than to the mutation itself.

The primary astrocytes produce endogenous wild-type GFAP, which could influence the polymerization of the mutant GFAP. They also contain vimentin, which can co-polymerize with GFAP (Parry and Steinert, 1999). We therefore expressed the mutant GFAP in Cos-7 cells, which contain vimentin but not GFAP, and in SW13Vim⁻ cells, which contain no endogenous cytoplasmic intermediate filaments (Hedberg and Chen, 1986). When transfected into Cos-7 cells, both the wild-type and mutant GFAPs integrated into intermediate filaments with vimentin (Fig. 1D, arrow, Fig. 1E), and also formed aggregates (Fig. 1D, arrowhead, Fig. 1F) similar to those observed in rat primary astrocytes.

When transfected in SW13Vim⁻ cells, wild-type GFAP formed thick and thin filamentous structures that spread throughout the cytoplasm (Fig. 2A,B). Occasionally an additional 'diffuse' cytoplasmic labeling was observed (Fig. 2B). By contrast, mutant GFAP was not organized into filament networks or bundles but was found in an 'irregular' pattern of small clumps scattered throughout the cytoplasm, superimposed upon a 'diffuse' cytoplasmic staining pattern (data not shown). To examine these structures further, we used confocal microscopy, taking 1 μm optical sections. Observed

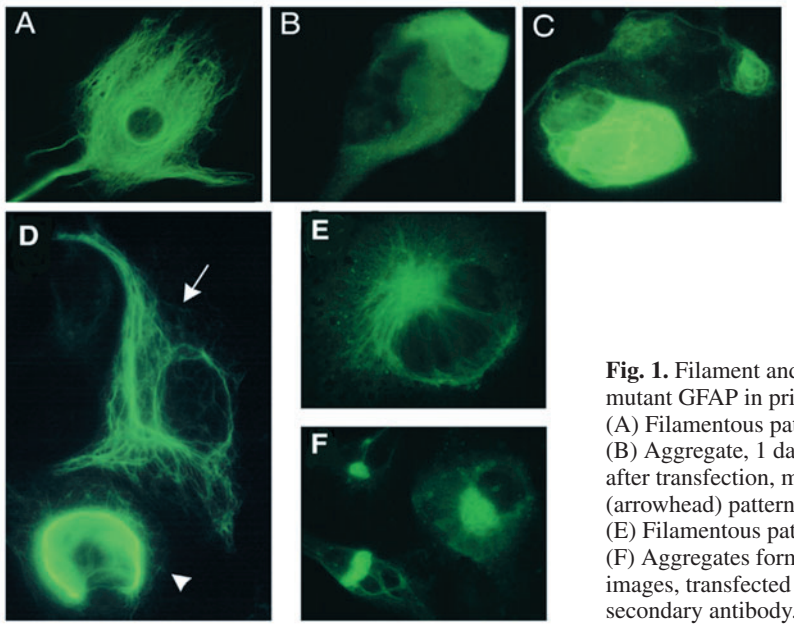

Fig. 1. Filament and aggregate patterns after the production of wild-type or mutant GFAP in primary rat astrocytes (A-C) and Cos-7 cells (D-F). (A) Filamentous pattern, 1 day after transfection, wild-type GFAP. (B) Aggregate, 1 day after transfection, wild-type GFAP. (C) Aggregate, 1 day after transfection, mutant GFAP. (D) Filamentous (arrow) and aggregate (arrowhead) patterns formed by wild-type GFAP at 3 days after transfection. (E) Filamentous pattern formed by mutant GFAP at 1 day after transfection. (F) Aggregates formed by mutant GFAP at 3 days after transfection. In all images, transfected GFAP was visualized with SMI21 and a FITC-conjugated secondary antibody. Magnification 900× for all images.

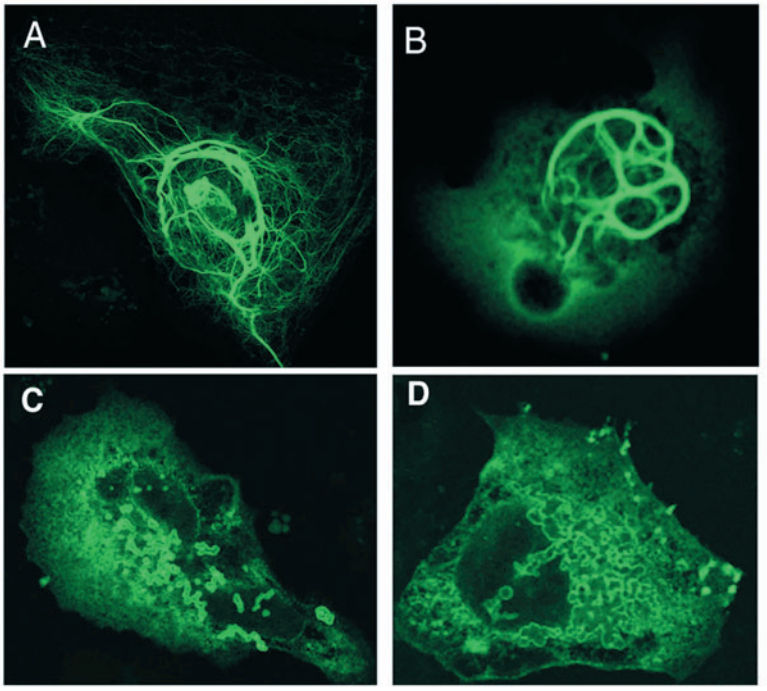

Fig. 2. Filamentous and irregular patterns after expression of wild-type (A,B) and mutant GFAP (C,D) in SW13Vim$^-$ cells. (A) Filamentous pattern, 1 day after transfection with wild-type. (B) Filamentous pattern with 'diffuse' background 1 day after transfection with wild-type GFAP, visualized with ALD-10, an anti-panGFAP antibody, and a FITC-conjugated secondary antibody. (C) Irregular pattern, 1 day after transfection with mutant GFAP. (D) 3 days after transfection with mutant. GFAP was visualized with SMI21 and a FITC-conjugated secondary antibody. All images represent 1 μm confocal optical sections. Magnification 900× for all images.

in this way, the small clumps resembled bent and twisted bundles that often appeared to fold back on themselves (Fig. 2C,D). Other structures, near the edges of the cells, appeared solid (Fig. 2D). These were visible at both 1 day and 3 days after transfection.

Mutant GFAPs incorporate into filament networks after transfection into astrocytes and Cos-7 cells but not SW13Vim$^-$ cells, suggesting that the mutant GFAPs can coassemble with wild-type GFAP or vimentin but cannot form intermediate-filament networks on their own. To test the ability of wild-type GFAP to rescue R239C GFAP to form an intermediate-filament network, wild-type and R239C GFAP were co-transfected into SW13Vim$^-$ cells. This resulted in some filamentous networks but also a range of other patterns, including 'diffuse' or 'irregular' distributions of GFAP (Fig. 3A-D).

Statistical analyses of the various patterns observed for the transfection of either wild-type or R239C GFAP into SW13Vim$^-$ cells revealed several important trends. 1 day after transfection, wild-type GFAP formed filament networks (Fig. 4A) and, although some of the cells contained 'diffuse' patterns, these were always accompanied by a filament network. By contrast, the R239C GFAP never formed filamentous networks but cells were instead about evenly divided between those that showed only a 'diffuse' pattern (57.8%) and those with an irregular pattern as well as the 'diffuse' pattern (42.1%).

Co-transfection of wild-type GFAP with the R239C GFAP ('wt+m') had a dramatic influence upon these phenotypes; for example, the proportion of cells with an exclusively 'diffuse' pattern decreased to 14.4% from the 57.8% observed with mutant GFAP alone (P=0.00026, by Student's t test) at 1 day after transfection. Many transfected cells had GFAP networks: 2.0% formed filaments exclusively, whereas about 27% formed filaments in the presence of a 'diffuse' background.

The patterns observed 3 days after transfection (Fig. 4B) were similar to those 1 day after transfection. Upon co-transfection with the wild-type and mutant GFAPs, the proportion of cells with a 'diffuse' pattern fell even further compared with the 1 day after transfection data (P=4.5×10^{-4} compared with mutant alone by Student's t test), and there was a corresponding increase in cells displaying filaments either exclusively or together with other patterns. A new combination also appeared, in which cells contained both filaments and an irregular pattern but without the 'diffuse' background.

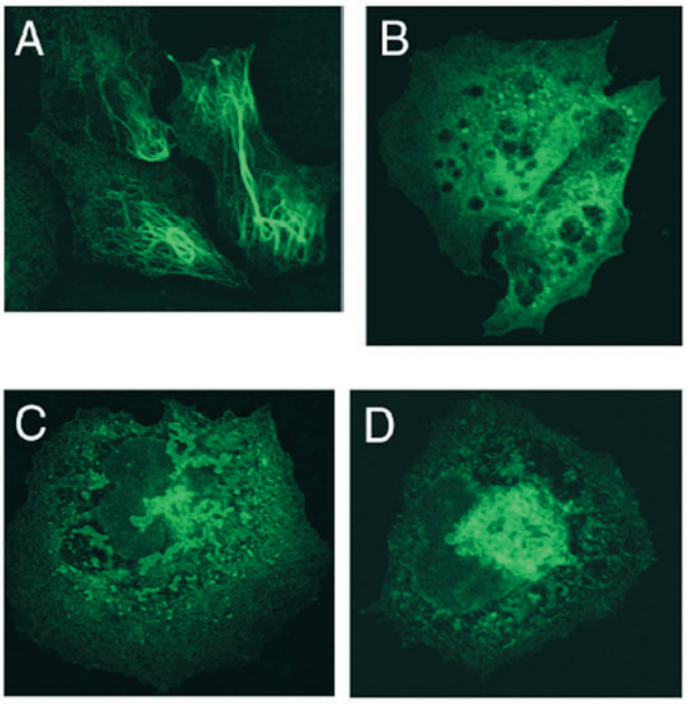

Solubility properties of GFAP in SW13Vim$^-$ cells

We wanted to know whether the mutant GFAP in 'diffuse' and irregular patterns in SW13Vim$^-$ cells had different solubility

Fig. 3. Filamentous, 'irregular' and 'diffuse' patterns 1 day after co-transfection of wild-type and mutant GFAP in SW13Vim$^-$ cells. Filamentous (A), 'diffuse' (B) and irregular with a 'diffuse' background (C,D) patterns are shown. All images represent 1 μm confocal optical sections. GFAP was visualized with ALD-10 and a FITC-conjugated secondary antibody. Magnification 900× for all images.

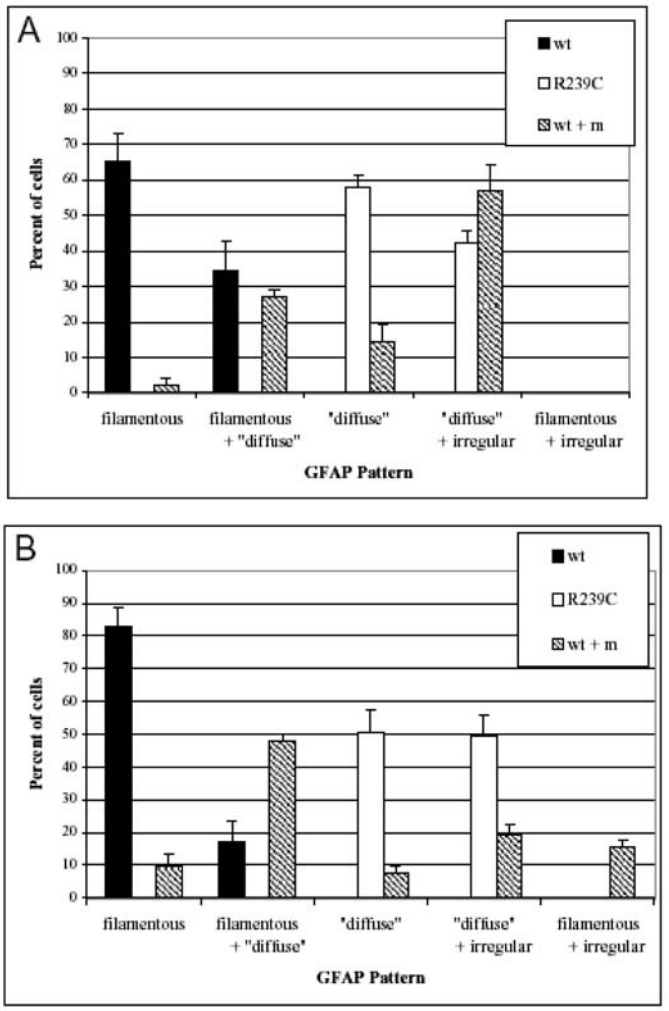

Fig. 4. Distributions of patterns after transfection of wild-type and mutant GFAPs into SW13Vim$^-$ cells. (A) 1 day after transfection. (B) 3 days after transfection. For each plasmid and time point, cells on three or four coverslips were counted and assigned to a category based on their appearance with standard fluorescence microscopy, using a 100× oil objective. The mean proportions of cells with each pattern type are shown, along with error bars representing one standard deviation. R239C, mutant; wt, wild type; wt + m, co-transfection of wild-type and mutant GFAP plasmids. The difference between the proportion of cells with an exclusively 'diffuse' pattern 1 day after transfection of mutant GFAP alone (57.8%) versus after co-transfection of wild-type and mutant GFAP (14.4%) is significant with a P value of 2.6×10^{-4} by Student's t test. After 3 days, the difference remains significant with a P value of 4.5×10^{-4} by Student's t test.

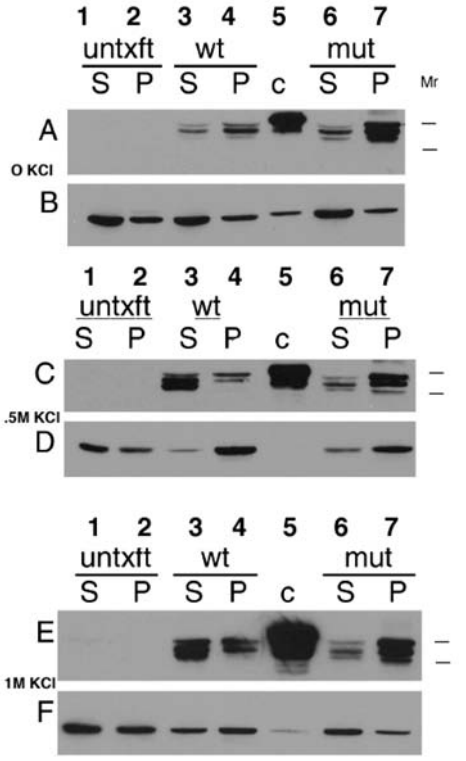

Fig. 5. Solubility properties of wild-type and mutant GFAPs produced in SW13Vim$^-$ cells and extracted with Triton X-100 buffer with increasing salt concentrations. Transfected SW13Vim$^-$ cells were extracted with a 0.5% Triton X-100 buffer without KCl (A,B) or with buffer also containing either 0.5 M KCl (C,D) or 1.0 M KCl (E,F). Nitrocellulose transfers were probed with an anti-GFAP antibody (Chemicon) (A,C,E) and then stripped and reprobed with an anti-actin antibody (B,D,F). Lanes: S, supernatant fraction; P, pellet fraction after centrifugation at 16,000 ***g***; untxft, untransfected cells; wt, wild-type GFAP; mut, mutant GFAP; c, Triton-X-100-insoluble fraction from primary rat astrocytes, as positive control. Mr, molecular weight markers (60 kDa and 40 kDa).

properties from those of wild-type GFAP. The high transfection efficiency of SW13Vim$^-$ cells enabled detection of the GFAP by western blotting. GFAP monomers and short polymers were separated from larger structures by extraction with buffer containing 0.5% Triton X-100 followed by centrifugation at 16,000 ***g*** for 10 minutes at 4°C (Goldman and Abramson, 1990). Extractions were done 1 day after transfection and the lysates analysed by SDS-PAGE (Fig. 5). After the transfection of either wild-type or mutant GFAP alone, the protein was found in both the Triton-soluble and the Triton-insoluble fractions (Fig. 5A). We then tested the solubility of the GFAPs in the presence of high salt, which has been used to measure the stability of intermediate-filament-associated protein interactions (Foisner et al., 1995; Gall et al., 1989; Ouyang and Sugrue, 1992). When 0.5 M KCl was added to the 0.5% Triton X-100 extraction buffer, much of the wild-type GFAP no longer sedimented but instead appeared in the supernatant under the conditions of our assay (Fig. 5C, lanes 3,4). By contrast, the mutant GFAP remained unchanged in its distribution between the two fractions (Fig. 5C, lanes 6,7). When 1.0 M KCl was added to the 0.5% Triton X-100 buffer, the wild-type GFAP remained largely in the supernatant solution (Fig. 5E, lanes 3, 4) but the mutant GFAP still remained little changed in its distribution (Fig. 5E, lanes 6,7).

Although most GFAP was found in one primary band, smaller proteins were also identified by our anti-GFAP antibody, and these are consistent with GFAP breakdown products (Dahl and Bignami, 1975). There were no higher-molecular-weight bands that would suggest multimerization stable to SDS (not shown).

When cells were transfected with both wild-type and mutant GFAP together and then extracted 1 day after transfection with 0.5 M KCl added to the 0.5% Triton X-100 buffer, the GFAP partitioned between fractions identically to the mutant form (data not shown). Thus, the mutant GFAP has a dominant effect over the wild type with respect to solubility.

The blots were stripped and reprobed with an anti-actin antibody as a further control for the numbers of cells extracted and the amount of total protein loaded on each gel. The amount of actin was similar in each of the soluble fractions and each of the pellet fractions (Fig. 5B,D,F).

In vitro assembly and electron microscopy

To investigate further the assembly properties of mutant GFAP, we used in vitro conditions to induce filament formation and visualized the resulting polymers by electron microscopy after negatively staining the samples. Both the wild-type GFAP (Fig. 6A) and the R239C GFAP (Fig. 6B) formed 10 nm filaments that were very similar at this gross morphological level. The ability of the R239C GFAP to form filaments in vitro suggests that the differences observed between wild-type and R239C GFAP by transfection is probably not caused by compromised assembly. Rather, the formation of the irregular patterns in vivo and the resistance to high salt extraction might be due to an association of the R239C GFAP with other intracellular proteins that are found on intermediate filaments (Quinlan, 2002) or abnormal interfilament interactions.

Sedimentation assay

To compare the relative efficiencies of polymerization of the wild-type and R239C GFAPs, the in-vitro-assembled GFAP samples were separated into pellet and supernatant fractions by centrifugation and assayed by SDS-PAGE. There was a higher proportion of R239C GFAP in the pellet fraction (Fig. 7, lanes 3,4) than of the wild type (Fig. 7, lanes 1,2). When the mutant and wild type were mixed in a 1:1 ratio, the pellet fraction again had higher levels than wild-type GFAP alone (Fig. 7, lanes 5,6). These data show that the mutant GFAP sediments more efficiently than wild-type GFAP and that this effect is dominant over the wild type. These results could be explained by the R239C GFAP having increased filament stability and/or increased interfilament interactions.

Discussion

We have used transient transfection of several different cell types to compare the properties of wild-type human GFAP to the protein containing the R239C Alexander-disease mutation. Cell types used were primary rat astrocytes, which contain both GFAP and vimentin; Cos-7 cells, which contain vimentin; and SW13Vim$^-$ cells, which contain no endogenous cytoplasmic intermediate filaments. Both wild-type and mutant GFAP incorporated into intermediate-filament structures in primary astrocytes and Cos-7 cells, both of which contain endogenous coassembly partners such as GFAP and/or vimentin (Quinlan and Franke, 1983). The wild-type GFAP was also able to form filament bundles in the SW13Vim$^-$ cells but the R239C GFAP only formed irregular, twisted and curly profiles, or gave only a ‘diffuse’ pattern of staining. However, like the wild-type protein, the large majority of the mutant GFAP resided in a low-speed Triton-X-100-insoluble fraction, indicating that it is apparently able to polymerize or form aggregates. Indeed, our in vitro assembly and electron microscopy demonstrated that the mutant protein formed 10 nm filaments that were morphologically similar to wild-type filaments.

The mutation does not, therefore, disrupt those interactions that allow a filament to form or allow subunits to associate together. This is consistent with previous studies on rod point mutations in lamin A and keratin K14, which did not disrupt tetramerization (Heald and McKeon, 1990; Letai et al., 1992). This suggests that, if the overall heptad repeats are preserved, tetramers and probably higher-order filamentous polymers can be formed (Meng et al., 1994). In fact, the GFAP mutation appears to have conferred increased stability on the assembled protein, as judged by its lowered solubility at high salt concentrations.

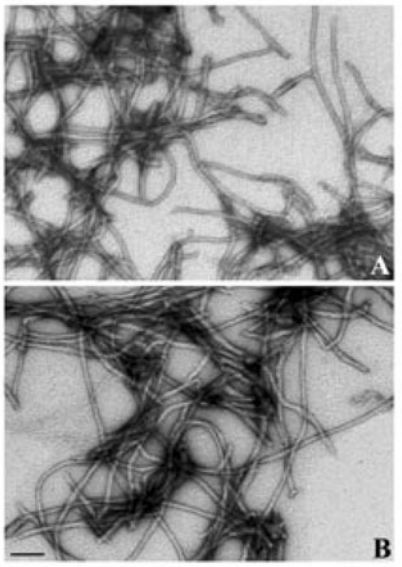

Fig. 6. Electron microscopy of in-vitro-assembled wild-type and mutant GFAP. Recombinant wild-type (A) and mutant (B) GFAP were assembled in vitro as described. Notice that both samples contain intermediate sized filaments (~10 nm) that are morphologically similar. Scale bars, 100 nm.

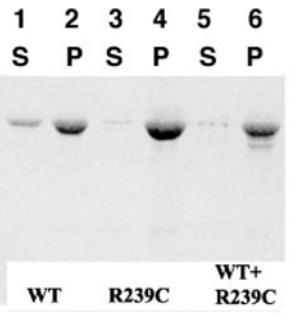

Fig. 7. Sedimentation assays. Recombinant human wild-type GFAP (WT) and mutant GFAP (R239C) were purified and assembled individually or as a 1:1 (WT+R239C) mixture at 0.5 mg ml^{-1}. After assembly, the samples were centrifuged and the supernatant (S) and pellet (P) fractions analysed by SDS-PAGE.

The irregular pattern seen in SW13Vim$^-$ cells transfected by mutant GFAP suggests that the mutation affects the organization of de novo GFAP networks and the ability to assemble robustly in the absence of wild-type GFAP and vimentin. R239C GFAP is, however, capable of assembly in vitro, forming 10 nm filaments morphologically similar to those formed by wild-type GFAP. By in vitro sedimentation assay, however, the R239C GFAP filaments sedimented more efficiently than the wild-type filaments, suggesting that there are probably changes in filament properties. In the context of the cell, a difference was found between the extractabilities of R239C and wild-type GFAP. The irregular structures and resistance to salt extraction could arise from aberrant filament-filament interactions. These changes in the properties of the mutant protein could result from a direct effect of the mutation on the overall filament architecture or on its interactions with other cellular constituents. Also possible is an indirect effect through an alteration in post-translational modification, although this would not explain the changes in cell-free polymerization, which used proteins generated in bacteria.

Patients affected by Alexander disease are heterozygous for GFAP mutations (Li et al., 2002), and so the mutations act in a genetically dominant manner. Although we do not yet know the actual ratio of wild-type to mutant protein in the Alexander-disease brain, the data presented here are consistent with a dominant effect of the R239C mutation. Both co-transfection studies and the in vitro coassembly demonstrated the dominant nature of the R239 mutation over the wild type. The mutation also appeared to be dominant with respect to filament solubility at high salt concentrations, because the GFAP in the co-transfectants displayed a solubility pattern like that of the mutant GFAP alone. Finally, in the sedimentation assay, the mutant appeared to have a dominant effect on the assembly of wild-type GFAP.

It is clear that high expression of wild-type GFAP leads to inclusion formation in astrocytes. Transgenic mice overexpressing the human GFAP, driven by its own promoter, form Rosenthal fibers (Eng et al., 1998; Messing et al., 1998). The transfection of wild-type GFAP into astrocytes leads to the formation of intermediate-filament aggregates (Koyama and Goldman, 1999), although these inclusions do not fully resemble Rosenthal fibers. Furthermore, Rosenthal fibers are found in the brains of patients in areas of long-standing gliosis or within highly fibrillary gliomas, such as juvenile pilocytic astrocytomas. Presumably, few if any of these patients have mutations in *GFAP*, because none of them has Alexander disease. In Alexander disease itself, we do not know whether there is increased or decreased transcription of either the mutant or wild-type *GFAP*, as is sometimes caused by some lamin A (*LMNA*) mutations (Mounkes et al., 2003). However, steady state levels of wild type and mutant transcripts appear to be the same in brain tissues from one R239C patient (R. Tian, unpublished).

Relationship between mutations found in GFAP and those in other intermediate filaments

The evidence that the R239C mutation in GFAP changes the organization and solubility of the protein and filament network is underscored by the observation that the corresponding residues in vimentin, desmin and lamin A/C are also arginine, and so might play a crucial role in the assembly of filaments. Indeed, the L12 and 2A rod-domain regions flanking this residue are well conserved between GFAP, vimentin, desmin and peripherin (Quinlan et al., 1995). In vimentin, they are involved in intra- and intermolecular cross-links (Steinert et al., 1993; Steinert et al., 1999). They also play a role in determining subfilament architecture (Parry et al., 2001). Given that the R239C mutation in GFAP studied here is nonconservative, some distortion of the protein in the vicinity of the mutation is likely. Once structural information becomes available (Strelkov et al., 2002; Strelkov et al., 2003; Herrmann et al., 2003) and includes the L12 and 2A rod regions, the important intra- and interhelical salt bridges present in this region will help to identify more precisely the role of R239 in GFAP and the other intermediate-filament proteins.

A mutation exactly homologous to R239C has been found in the Type-V intermediate filament lamin A/C (Raffaele Di Barletta et al., 2000). Patients with this R249Q mutation have autosomal dominant Emery-Dreifuss muscular dystrophy, which presents with cardiac arrhythmias and muscle contractures (Raffaele Di Barletta et al., 2000). It has been hypothesized that mutations in lamin A/C affect the structure of the nuclear lamina and lead to changes in the distribution of emerin, a protein found in the inner nuclear membrane (Toniolo and Minetti, 1999; Hutchison, 2002). Structures homologous to Rosenthal fibers have been observed in myopathies caused by dominant mutations in desmin, an intermediate filament closely related to GFAP (Dalakas et al., 2000). These mutations result in intracellular inclusions in muscle composed of desmin, αB-crystallin and ubiquitin (Goebel and Warlo, 2000). At least one of the mutations, found in the 2B subdomain of the rod section, has been found to disturb the organization of desmin in both SW13Vim$^-$ cells and a myoblast cell line in patterns similar to those observed in this study (Goudeau et al., 2001).

Two striking differences between diseases caused by mutations in other intermediate-filament proteins such as the keratins (Irving and McLean, 1999) and the Alexander-disease mutations in GFAP are that a normal filament network fails to form in the other diseases, and that those disorders can be mimicked by null mutations in mice. In Alexander disease, however, the intermediate filaments surrounding Rosenthal fibers look normal and GFAP-null mice display neither the pathology nor the clinical signs of Alexander disease.

A deleterious effect of elevated GFAP levels per se has been indicated by studies in which mice expressing high levels of a wild-type human GFAP transgene died at 14-20 days of age and displayed large numbers of Rosenthal fibers in their astrocytes (Eng et al., 1998; Messing et al., 1998). By contrast, *GFAP*-knockout mice are relatively healthy, developing minor deficiencies only late in life (Gomi et al., 1995; Liedtke et al., 1996; Pekny et al., 1995; Shibuki et al., 1996). Thus, an increase in GFAP accumulation results in a pathological condition. Our finding that the R239C mutation increases GFAP structural stability is consistent with such an etiology for Alexander disease.

Additional research on the relationships between the locations of the other mutations found in Alexander-disease patients, the ability to form bundled filaments, the stability of mutant polymers and the age of onset and disease severity will elucidate the spectrum of effects of the mutations.

We are grateful to A. Messing and R. Liem for their assistance and many comments, and to T. Swayne for help with confocal microscopy. This work was supported by NIH grants EY09331 (J.E.G.), NS17125 (J.E.G.) and NS42803 (M.B., R.A.Q. and J.E.G.). V.C.H. was supported by the Medical Scientist Training Program at Columbia University (GM07367).

References

Alexander, W. S. (1949). Progressive fibrinoid degeneration of fibrillary astrocytes associated with mental retardation in a hydrocephalic infant. *Brain* **72**, 373-381.

Aoki, Y., Haginoya, K., Munakata, M., Yokoyama, H., Nishio, T., Togashi, N., Ito, T., Suzuki, Y., Kure, S., Iinuma, K. et al. (2001). A novel mutation in glial fibrillary acidic protein gene in a patient with Alexander disease. *Neurosci. Lett.* **312**, 71-74.

Bettica, A. and Johnson, A. B. (1990). Ultrastructural immunogold labeling of glial filaments in osmicated and unosmicated epoxy-embedded tissue. *J. Histochem. Cytochem.* **38**, 103-109.

Borrett, D. and Becker, L. E. (1985). Alexander's disease: a disease of astrocytes. *Brain* **109**, 367-385.

Brenner, M., Lampel, K., Nakatani, Y., Mill, J., Banner, C., Mearow, K., Dohadwala, M., Lipsky, R. and Freese, E. (1990). Characterization of human cDNA and genomic clones for glial fibrillary acidic protein. *Mol. Brain Res.* **7**, 277-286.

Brenner, M., Johnson, A. B., Boespflug-Tanguy, O., Rodriguez, D., Goldman, J. E. and Messing, A. (2001). Mutations in *GFAP*, encoding glial fibrillary acidic protein, are associated with Alexander disease. *Nat. Genet.* **27**, 117-120.

Chin, S. S. M. and Liem, R. H. K. (1989). Expression of rat neurofilament proteins NF-L and NF-M in transfected non-neuronal cells. *Eur. J. Cell Biol.* **50**, 475-490.

Dahl, D. and Bignami, A. (1975). Glial fibrillary acidic protein from normal and gliosed human brain. Demonstration of multiple related polypeptides. *Biochim. Biophys. Acta* **386**, 41-51.

Dalakas, M. C., Park, K. Y., Semino-Mora, C., Lee, H. S., Sivakumar, K. and Goldfarb, L. G. (2000). Desmin myopathy, a skeletal myopathy with cardiomyopathy caused by mutations in the desmin gene. *New. Engl. J. Med.* **342**, 770-780.

Duckett, S., Schwartzman, R. J., Osterholm, J., Rorke, L. B., Friedman, D. and McLellan, T. L. (1992). Biopsy diagnosis of familial Alexander's disease. *Pediatr. Neurosurg.* **18**, 134-138.

Eng, L. F., Lee, Y. L., Kwan, H., Brenner, M. and Messing, A. (1998). Astrocytes cultured from transgenic mice carrying the added human glial fibrillary acidic protein gene contain Rosenthal fibers. *J. Neurosci. Res.* **53**, 353-360.

Foisner, R., Bohn, W., Mannweiler, K. and Wiche, G. (1995). Distribution and ultrastructure of plectin arrays in subclones of rat glioma C6 cells differing in intermediate filament protein (vimentin) expression. *J. Struct. Biol.* **115**, 304-317.

French, T. A., Bower, B. D. and Cameron, A. H. (1976). Alexander's disease presenting as astrocytoma. *J. Neurol. Neurosurg. Psych.* **39**, 803-809.

Friede, R. (1989). *Developmental Neuropathology*. New York: Springer-Verlag.

Gall, L., le Guen, P. and Huneau, D. (1989). Cytokeratin-like proteins in the sheep oocyte. *Cell Differ. Dev.* **28**, 95-104.

Goebel, H. H. and Warlo, I. (2000). Gene-related protein surplus myopathies. *Mol. Genet. Metab.* **71**, 267-275.

Goldman, J. E. and Abramson, B. J. (1990). Cyclic AMP-induced shape changes of astrocytes are accompanied by rapid depolymerization of actin. *Brain Res.* **528**, 189-196.

Goldman, J. E. and Chiu, F.-C. (1984). Growth kinetics, cell shape, and the cytoskeleton of primary astrocyte cultures. *J. Neurochem.* **42**, 175-184.

Goldman, J. E. and Corbin, E. (1988). Isolation of a major protein component of Rosenthal fibers. *Am. J. Pathol.* **130**, 569-578.

Gomi, H., Yokoyama, T., Fujimoto, K., Ikeda, T., Katoh, A., Itoh, T. and Itohara, S. (1995). Mice devoid of the glial fibrillary acidic protein develop normally and are susceptible to scrapie prions. *Cell* **14**, 29-41.

Gorospe, J. R., Naidu, S., Johnson, A. B., Puri, V., Raymond, G. V., Jenkins, S. D., Pedersen, R. C., Lewis, D., Knowles, P., Fernandez, R. et al. (2002). Molecular findings in symptomatic and pre-symptomatic Alexander disease patients. *Neurology* **58**, 1494-1500.

Goudeau, B., Dagvadorj, A., Rodrigues-Lima, F., Nedellec, P., Casteras-Simon, M., Perret, E., Langlois, S., Goldfarb, L. and Vicart, P. (2001). Structural and functional analysis of a new desmin variant causing desmin-related myopathy. *Hum. Mut.* **18**, 388-396.

Head, M. W., Corbin, E. and Goldman, J. E. (1994). Coordinate and independent regulation of alpha-B-crystallin and HSP27 expression in response to physiological stress. *J. Cell Physiol.* **159**, 41-50.

Heald, R. and McKeon, F. (1990). Mutations of phosphorylation sites in lamin A that prevent nuclear lamina disassembly in mitosis. *Cell* **61**, 579-589.

Hedberg, K. K. and Chen, L. B. (1986). Absence of intermediate filaments in a human adrenal cortex carcinoma-derived cell line. *Exp. Cell Res.* **163**, 509-517.

Henin, D., Hauw, J.-J. and Escourolle, R. (1986). Astrocytes in Alexander's disease. In *Astrocytes* (ed. S. Federoff and A. Vernadakis), pp. 387-400. Orlando: Academic Press.

Herndon, R. M., Rubinstein, L. J., Freeman, J. M. and Mathieson, G. (1970). Light and electron microscopic observations on Rosenthal fibers in Alexander's disease and in multiple sclerosis. *J. Neuropath. Exp. Neurol.* **29**, 524-551.

Herrmann, H., Hesse M., Reichenzeller M., Aebi U. and Magin, T. M. (2003). Functional complexity of intermediate filament cytoskeletons: from structure to assembly to gene ablation. *Int. Rev. Cytol.* **223**, 83-175.

Hutchison, C. J. (2002). Lamins: building blocks or regulators of gene expression? *Nat. Rev. Mol. Cell Biol.* **3**, 848-858.

Irving, A. D. and McLean, W. H. (1999). Human keratin diseases: the increasing spectrum of disease and subtlety of the phenotype-genotype correlation. *Br. J. Dermatol.* **140**, 815-828.

Iwaki, T., Kume-Iwaki, A., Liem, R. K. H. and Goldman, J. E. (1989). Alpha-B-crystallin is expressed in non-lenticular tissues and accumulates in Alexander's disease brain. *Cell* **57**, 71-78.

Johnson, A. B. and Bettica, A. (1989). On-grid immunogold labeling of glial intermediate filaments in epoxy-embedded tissue. *Am. J. Anat.* **185**, 335-341.

Koyama, Y. and Goldman, J. E. (1999). Formation of GFAP cytoplasmic inclusions in astrocytes and their disaggregation by alpha-B-crystallin. *Am. J. Pathol.* **154**, 1563-1572.

Lach, B., Sikorska, M., Rippstein, P., Gregor, A., Staines, W. and Davie, T. R. (1991). Immunoelectron microscopy of Rosenthal fibers. *Acta Neuropathol.* **81**, 503-509.

Letai, A., Coulombe, P. A. and Fuchs, E. (1992). Do the ends justify the mean? Proline mutations at the ends of the keratin coiled-coil rod segment are more disruptive than internal mutations. *J. Cell Biol.* **116**, 1181-1195.

Li, R., Messing, A., Goldman, J. E. and Brenner, M. (2002). GFAP mutations in Alexander disease. *Int. J. Dev. Neurosci.* **20**, 259-268.

Liedtke, W., Edelmann, W., Bieri, P. L., Chiu, F.-C., Cowan, N. J., Kucherlapati, R. and Raine, C. S. (1996). GFAP is necessary for the integrity of CNS white matter architecture and long-term maintenance of myelination. *Neuron* **17**, 607-615.

Lowe, J., Morrell, K., Lennox, G., Landon, M. and Mayer, R. J. (1989). Rosenthal fibers are based on the ubiquitination of glial filaments. *Neuropathol. Appl. Neurobiol.* **15**, 45-53.

Meng, J. J., Khan, S. and Ip, W. (1994). Charge interactions in the rod domain drive formation of tetramers during intermediate filament assembly. *J. Biol. Chem.* **269**, 18679-18685.

Messing, A., Head, M. W., Galles, K., Galbreath, E. J., Goldman, J. E. and Brenner, M. (1998). Fatal encephalopathy with astrocyte inclusions in *GFAP* transgenic mice. *Am. J. Path.* **152**, 391-398.

Mounkes L. C., Kozlov S., Hernandez L., Sullivan T. and Stewart, C. L. (2003). A progeroid syndrome in mice is caused by defects in A-type lamins. *Nature* **423**, 298-301.

Okamoto, Y., Mitsuyama, H., Jonosono, M., Hirata, K., Arimura, K., Osame, M. and Nakagawa, M. (2002). Autosomal dominant palatal myoclonus and spinal cord atrophy. *J. Neurol. Sci.* **195**, 71-76.

Ouyang, P. and Sugrue, S. P. (1992). Identification of an epithelial protein related to the desmosome and intermediate filament network. *J. Cell Biol.* **118**, 1477-1488.

Parry, D. A. and Steinert, P. M. (1999). Intermediate filaments: molecular architecture, assembly, dynamics and polymorphism. *Q. Rev. Biophys.* **32**, 99-187.

Parry, D. A., Marekov, L. N. and Steinert, P. M. (2001). Subfilamentous protofibril structures in fibrous proteins: cross-linking evidence for protofibrils in intermediate filaments. *J. Biol. Chem.* **276**, 39253-39258.

Pekny, M., Leveen, P., Pekna, M., Eliasson, C., Berthold, C.-H.,

Westermark, B. and Betsholtz, C. (1995). Mice lacking glial fibrillary acidic protein display astrocytes devoid of intermediate filaments but develop and reproduce normally. *EMBO J.* **14**, 1590-1598.

Perng, M. D., Cairns, L., van den IJssel, P., Prescott, A., Hutcheson, A. M. and Quinlan, R. A. (1999). Intermediate filament interactions can be altered by HSP27 and alpha-B-crystallin. *J. Cell Sci.* **112**, 2099-2112.

Quinlan, R. (2002). Cytoskeletal competence requires protein chaperones. *Prog. Mol. Subcell. Biol*. **28**, 219-233.

Quinlan, R. A. and Franke, W. W. (1983). Molecular interactions in intermediate-sized filaments revealed by chemical cross-linking. Heteropolymers of vimentin and glial filament protein in cultured human glioma cells. *Eur. J. Biochem*. **16**, 477-484.

Quinlan, R., Hutchison, C. and Lane, B. (1995). Intermediate filament proteins. *Protein Profile* **2**, 795-952.

Raffaele di Barletta, M., Ricci, E., Galluzzi, G., Tonali, P., Mora, M., Morandi, L., Romorini, A., Voit, T., Orstavik, K. H., Merlini, L. et al. (2000). Different mutations in the *LMNA* gene cause autosomal dominant and autosomal recessive Emery-Dreifuss muscular dystrophy. *Am. J. Hum. Genet.* **66**, 1407-1412.

Ralton, J. E., Lu, X., Hutcheson, A. M. and Quinlan, R. A. (1994). Identification of two N-terminal non-alpha-helical domain motifs important in the assembly of glial fibrillary acidic protein. *J. Cell Sci.* **107**, 1935-1948.

Reichard, E. A. P., Ball, W. S. and Bove, K. E. (1996). Alexander disease: a case report and review of the literature. *Pediatr. Pathol. Lab. Med.* **16**, 327-343.

Rodriguez, D., Gauthier, F., Bertini, E., Bugiani, M., Brenner, M., N'guyen, S., Goizet, C., Gelot, A., Surtees, R., Pedespan, J. M. et al. (2001). Infantile Alexander disease: spectrum of *GFAP* mutations and genotype-phenotype correlation. *Am. J. Hum. Genet.* **69**, 1134-1140.

Rosner, B. (1990). *Fundamentals of Biostatistics*. Boston: PWS-Kent Publishing Company.

Sawaishi, Y., Hatazawa, J., Ochi, N., Hirono, H., Yano, T., Watanabe, Y., Okudera, T. and Takada, G. (1999). Positron emission tomography in juvenile Alexander disease. *J. Neurol. Sci.* **165**, 116-120.

Sawaishi, Y., Yano, T., Takaku, I. and Takada, G. (2002). Juvenile Alexander disease with a novel mutation in glial fibrillary acidic protein gene. *Neurology* **58**, 1541-1543.

Shibuki, K., Gomi, H., Chen, L., Bao, S., Kim, J. J., Wakatsuki, H., Fujisaki, T., Ikeda, T., Chen, C., Thompson, R. F. et al. (1996). Deficient cerebellar long-term depression impaired eyeblink conditioning, and normal motor coordination in GFAP mutant mice. *Neuron* **16**, 587-599.

Shiihara, T., Kato, M., Honma, T., Ohtaki, S., Sawaishi, Y. and Hayasaka, K. (2002). Fluctuation of computed tomographic findings in white matter in Alexander's disease. *J. Child Neurol.* **17**, 227-230.

Shiroma, N., Kanazawa, N., Izumi, M., Sugai, K., Fukumizu, M., Sasaki, M., Hanaoka, S., Kaga, M. and Tsujino, S. (2001). Diagnosis of Alexander disease in a Japanese patient by molecular genetic analysis. *J. Hum. Genet.* **46**, 579-582.

Steinert, P. M., Marekov, L. N. and Parry, D. A. (1993). Diversity of intermediate filament structure. Evidence that the alignment of coiled-coil molecules in vimentin is different from that in keratin intermediate filaments. *J. Biol. Chem.* **268**, 24916-24925.

Steinert, P. M., Marekov, L. N. and Parry, D. A. (1999). Molecular parameters of type IV alpha-internexin and type IV-type III alpha-internexin-vimentin copolymer intermediate filaments. *J. Biol. Chem.* **274**, 1657-1666.

Strelkov, S. V., Herrmann, H., Geisler, N., Wedig, T., Zimbelmann, R., Aebi, U. and Burkhard, P. (2002). Conserved segments 1A and 2B of the intermediate filament dimer: their atomic structures and role in filament assembly. *EMBO J.* **21**, 1255-1266.

Strelkov, S. V., Herrmann, H. and Aebi, U. (2003). Molecular architecture of intermediate filaments. *BioEssays* **25**, 243-251.

Tomokane, N., Iwaki, T., Tateishi, J., Iwaki, A. and Goldman, J. (1991). Rosenthal fibers share epitopes with alpha-B-crystallin, glial fibrillary acidic protein, and ubiquitin, but not with vimentin: immunoelectron microscopy with colloidal gold. *Am. J. Pathol.* **138**, 875-885.

Toniolo, D. and Minetti, C. (1999). Muscular dystrophies: alteration in a limited number of cellular pathways? *Curr. Opin. Genet. Dev.* **9**, 275-282.

Journal of Cell Science